Near-threshold η production in pp collisions [*]

LÜ Qi-Fang(吕齐放)   LI De-Min(李德民)[1)]

Department of Physics, Zhengzhou University, Zhengzhou 450001, China

Abstract: We study near-threshold η meson production in pp collisions within an effective Lagrangian approach combined with the isobar model, by allowing for the various intermediate nucleon resonances due to the π, η, and ρ-meson exchanges. It is shown that the ρ-meson exchange is the dominant excitation mechanism for these resonances, and the contribution from the $N^*(1720)$ is dominant. The total cross section data can be reasonably reproduced, and the anisotropic angular distributions of the emitted η meson are consistent with experimental measurements. Besides, the invariant mass spectra of pp and pη explain the data well at excess energy of 15 MeV, and are basically consistent with the data at excess energy of 40 MeV. However, our model calculations cannot reasonably account for the two-peak structure in the pη distribution at excess energies of 57 and 72 MeV, which suggests that a more complicated mechanism is needed at higher energy region.

Key words: effective Lagrangian approach, isobar model, nucleon resonances

PACS: 13.75.Cs, 14.20.Gk, 13.30.Eg   **DOI:** 10.1088/1674-1137/39/11/113104

1   Introduction

The properties of hadrons are subject to the behavior of quantum chromodynamics (QCD) in the non-perturbative region, so the study of hadrons is important to deepen the understanding of the non-perturbative properties of QCD. Meson production reactions in nucleon–nucleon collisions near threshold are a good platform to obtain new information on the hadrons and therefore have received a lot of attention both experimentally and theoretically in recent years [1]. A large set of experimental data on η meson production in the pp→ppη [2–10], pn→dη, and pn→pnη reactions [11–14] has been accumulated, which has stimulated many theoretical investigations on η meson production [15–34].

η meson production in NN collisions is generally assumed to occur predominantly through re-scattering of the intermediate nucleon resonances caused by the meson exchanges. For this basic mechanism, it is not yet clear which of the possible nucleon resonances plays the dominant role. For example, in Refs. [15–19, 22–28] it is suggested that the $N^*(1535)$ is dominant, while in Ref. [33] it is found that the $N^*(1520)$ is dominant and the $N^*(1535)$ contribution is small due to the strong destructive interference among the exchanged mesons. Also, it is not yet clear which of the possible meson exchanges plays the most important role. For example, in Refs. [15, 22, 32] it is claimed that the pseudoscalar mesons π and η ex-

changes are dominant, whereas in Refs. [16, 19, 24, 25] it is suggested that vector meson ρ exchange is dominant. In Ref. [27] it is found that both the π exchange and the ρ exchange can describe the cross sections well. The study on the $N^*(1535)N\rho$ coupling in the framework of an effective Lagrangian approach shows that the value of $g_{N^*(1535)N\rho}$ is strong [35], which favors the importance of the ρ meson exchange in NN collisions.

In Ref. [34], the final state interaction (FSI) enhancement factor is considered and it is found that the measured pp and ηp effective mass spectra can be well reproduced by allowing for a linear energy dependence in the leading $^3P_0 \rightarrow {}^1S_0$, s partial wave amplitude.

In Ref. [8] it is suggested that the higher partial waves may be important even at 15.5 MeV. Besides the $N^*(1535)$, the ρ meson may also couple strongly to other higher resonances. The large branching ratio and the small phase space for the $N^*(1720) \rightarrow N\rho$ also suggest that the $N^*(1720)N\rho$ coupling is strong.

With the inspiration of the factors mentioned above, we shall re-study the pp → ppη reaction in an effective Lagrangian approach combined with the isobar model. The combination of the effective Lagrangian approach and the isobar model turns out to be a good method to study hadron resonance production in the πN, NN, and $\bar{K}$N scattering [22, 32, 33, 35–40]. In the present work, we assume that the near threshold η meson production in proton–proton collisions is through the intermediate

N*(1535), N*(1650), N*(1710), N*(1720), and the nucleon pole caused by the π, η, and ρ mesons exchanges. The proton–proton FSI and proton–η FSI are also considered.

This work is organized as follows. The basic formalism and ingredients used in our model are given in Section 2. The numerical results and discussions are given in Section 3. A summary is given in Section 4.

2　Formalism and ingredients

The basic tree-level Feynman diagrams for the pp→ppη reaction are shown in Fig. 1.
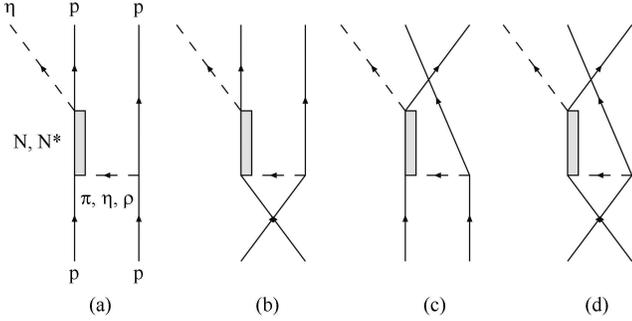
Fig. 1.　Feynman diagrams for the pp→ppη reaction.

The interaction Lagrangians for the πNN, ηNN and ρNN couplings can be written as [36, 37]:

$$\mathcal{L}_{\pi NN} = -\mathrm{i}g_{\pi NN}\bar{\psi}_N\gamma_5\vec{\tau}\cdot\vec{\pi}\psi_N, \tag{1}$$

$$\mathcal{L}_{\eta NN} = -\mathrm{i}g_{\eta NN}\bar{\psi}_N\gamma_5\eta\psi_N, \tag{2}$$

$$\mathcal{L}_{\rho NN} = -g_{\rho NN}\bar{\psi}_N\left(\gamma_\mu+\frac{\kappa}{2m_N}\sigma_{\mu\nu}\partial^\nu\right)\vec{\tau}\cdot\vec{\rho}^\mu\psi_N. \tag{3}$$

The effects of the non-point-like structures of exchanged mesons are taken into account by introducing the following off-shell form factors in the MNN vertexes [41–43]

$$F_M^{NN}(k_M^2)=\left(\frac{\Lambda_M^2-m_M^2}{\Lambda_M^2-k_M^2}\right)^n, \tag{4}$$

where M denotes the exchanged meson; $n=1$ for π^0NN and ηNN vertexes, $n=2$ for the ρ^0NN vertex; k_M, m_M, and Λ_M are the 4-momentum, mass, and cut-off parameter, respectively, for the exchanged-meson M. The relevant parameters used in our calculations are: $g_{\pi NN}^2/4\pi=14.4$, $g_{\eta NN}^2/4\pi=0.4$, $g_{\rho NN}^2/4\pi=0.9$, $\kappa=6.1$ [36, 37, 41–48], $\Lambda_\rho=1.85$ GeV [36, 37], and $\Lambda_\pi=\Lambda_\eta=0.8$ GeV.

The following interaction Lagrangians involving the nucleon resonances N* can be obtained within a Lorentz covariant orbital-spin (L-S) scheme for the N*NM couplings [49]:

$$\mathcal{L}_{\pi NN^*(1535)} = \mathrm{i}g_{\pi NN^*(1535)}\bar{\psi}_N\vec{\tau}\cdot\vec{\pi}\psi_{N^*(1535)}+\mathrm{h.c.}, \tag{5}$$

$$\mathcal{L}_{\eta NN^*(1535)} = \mathrm{i}g_{\eta NN^*(1535)}\bar{\psi}_N\eta\psi_{N^*(1535)}+\mathrm{h.c.}, \tag{6}$$

$$\mathcal{L}_{\rho NN^*(1535)} = \mathrm{i}g_{\rho NN^*(1535)}\bar{\psi}_N\gamma_5\left(\gamma_\mu-\frac{q_\mu\slashed{q}}{q^2}\right)$$
$$\times\vec{\tau}\cdot\vec{\rho}^\mu(p_\rho)\psi_{N^*(1535)}+\mathrm{h.c.}, \tag{7}$$

$$\mathcal{L}_{\pi NN^*(1650)} = \mathrm{i}g_{\pi NN^*(1650)}\bar{\psi}_N\vec{\tau}\cdot\vec{\pi}\psi_{N^*(1650)}+\mathrm{h.c.}, \tag{8}$$

$$\mathcal{L}_{\eta NN^*(1650)} = \mathrm{i}g_{\eta NN^*(1650)}\bar{\psi}_N\eta\psi_{N^*(1650)}+\mathrm{h.c.}, \tag{9}$$

$$\mathcal{L}_{\rho NN^*(1650)} = \mathrm{i}g_{\rho NN^*(1650)}\bar{\psi}_N\gamma_5\left(\gamma_\mu-\frac{q_\mu\slashed{q}}{q^2}\right)$$
$$\times\vec{\tau}\cdot\vec{\rho}^\mu(p_\rho)\psi_{N^*(1650)}+\mathrm{h.c.}, \tag{10}$$

$$\mathcal{L}_{\pi NN^*(1710)} = -\mathrm{i}g_{\pi NN^*(1710)}\bar{\psi}_N\gamma_5\vec{\tau}\cdot\vec{\pi}\psi_{N^*(1710)}+\mathrm{h.c.}, \tag{11}$$

$$\mathcal{L}_{\eta NN^*(1710)} = -\mathrm{i}g_{\eta NN^*(1710)}\bar{\psi}_N\gamma_5\eta\psi_{N^*(1710)}+\mathrm{h.c.}, \tag{12}$$

$$\mathcal{L}_{\rho NN^*(1710)} = -g_{\rho NN^*(1710)}\bar{\psi}_N\left(\gamma_\mu+\frac{\kappa}{2m_N}\sigma_{\mu\nu}\partial^\nu\right)$$
$$\times\vec{\tau}\cdot\vec{\rho}^\mu\psi_{N^*(1710)}+\mathrm{h.c.}, \tag{13}$$

$$\mathcal{L}_{\pi NN^*(1720)} = g_{\pi NN^*(1720)}\bar{\psi}_N\vec{\tau}\cdot\partial^\mu\vec{\pi}\psi_{N^*(1720)\mu}+\mathrm{h.c.}, \tag{14}$$

$$\mathcal{L}_{\eta NN^*(1720)} = g_{\eta NN^*(1720)}\bar{\psi}_N\partial^\mu\eta\psi_{N^*(1720)\mu}+\mathrm{h.c.}, \tag{15}$$

$$\mathcal{L}_{\rho NN^*(1720)} = g_{\rho NN^*(1720)}\bar{\psi}_N\gamma_5\vec{\tau}\cdot\vec{\rho}^\mu\psi_{N^*(1720)\mu}+\mathrm{h.c.}. \tag{16}$$

At the N*NM vertexes, the monopole form factors are employed:

$$F_M^{N^*N}(k_M^2)=\frac{\Lambda_M^{*2}-m_M^2}{\Lambda_M^{*2}-k_M^2}. \tag{17}$$

With the effective Lagrangians listed above, the partial width of the nucleon resonance N* can be derived. From the experimental data on the partial width of the corresponding nucleon resonance, the N*NM coupling constants can be obtained. For the N* resonance below the Nρ threshold, the partial decay width $\Gamma_{N^*\to N\rho\to N\pi\pi}$ is employed to determine the N*Nρ coupling constant [36, 37]. The relevant coupling constants and cut-off parameters are listed in Table 1.

For the nucleon pole N and nucleon resonances N*, the following form factors are used [37, 51–53]:

$$F_N(q^2) = \frac{\Lambda_N^4}{\Lambda_N^4+(q^2-m_N^2)^2}, \tag{18}$$

$$F_{N^*}(q^2) = \frac{\Lambda_{N^*}^4}{\Lambda_{N^*}^4+(q^2-M_{N^*}^2)^2}, \tag{19}$$

Table 1.   Relevant parameters of the nucleon resonances used in our calculation. The widths and branching ratios are taken from the PDG [50].

resonance	width/GeV	decay channel	branching ratios	$g^2/4\pi$	cut-off/GeV
N*(1535)	0.15	Nπ	0.45	0.037	0.8
		Nη	0.42	0.28	0.8
		Nρ	0.02	5.55	0.8
N*(1650)	0.15	Nπ	0.70	0.052	1.5
		Nη	0.10	0.036	1.5
		Nρ	0.01	0.0064	1.5
N*(1710)	0.1	Nπ	0.125	0.072	1.5
		Nη	0.20	0.97	1.5
		Nρ	0.15	0.019	1.5
N*(1720)	0.25	Nπ	0.11	0.11	1.5
		Nη	0.04	0.35	1.5
		Nρ	0.775	635.11	1.5

with $\Lambda_{\mathrm{N}}=1.0$ GeV and $\Lambda_{\mathrm{N}^*}=2.0$ GeV.

The meson propagators used in our calculation are:

$$G_{\pi/\eta}(k_{\pi/\eta}) = \frac{\mathrm{i}}{k_{\pi/\eta}^2 - m_{\pi/\eta}^2}, \tag{20}$$

$$G_\rho^{\mu\nu}(k_\rho) = -\mathrm{i}\left(\frac{g^{\mu\nu} - k_\rho^\mu k_\rho^\nu / k_\rho^2}{k_\rho^2 - m_\rho^2}\right). \tag{21}$$

The propagators of the N* resonances can be written as

$$G_{\mathrm{N}^*}(q) = \frac{\not{q} + M_{\mathrm{N}^*}}{q^2 - M_{\mathrm{N}^*}^2 + \mathrm{i}M_{\mathrm{N}^*}\Gamma_{\mathrm{N}^*}}, \tag{22}$$

for spin-$\frac{1}{2}$ resonances, and

$$G_{\mathrm{N}^*}^{\mu\nu}(q) = \frac{-P_{\mu\nu}(q)}{q^2 - M_{\mathrm{N}^*}^2 + \mathrm{i}M_{\mathrm{N}^*}\Gamma_{\mathrm{N}^*}}, \tag{23}$$

with

$$P_{\mu\nu}(q) = -(\not{q} + M_{\mathrm{N}^*}) \times \left[g_{\mu\nu} - \frac{1}{3}\gamma_\mu\gamma_\nu - \frac{1}{3M_{\mathrm{N}^*}}(\gamma_\mu q_\nu - \gamma_\nu q_\mu)\right.$$

$$\left. - \frac{2}{3M_{\mathrm{N}^*}^2}q_\mu q_\nu\right], \tag{24}$$

for spin-$\frac{3}{2}$ resonances.

As usual, in Eq. (22) the following energy-dependent total width of the N*(1535) resonance, $\Gamma_{\mathrm{N}^*(1535)}(s)$, is employed [54],

$$\Gamma_{\mathrm{N}^*(1535)}(s) = \Gamma_{\mathrm{N}^*(1535)\to\mathrm{N}\pi}\frac{\rho_{\pi\mathrm{N}}(s)}{\rho_{\pi\mathrm{N}}(M_{\mathrm{N}^*(1535)}^2)}$$

$$+ \Gamma_{\mathrm{N}^*(1535)\to\mathrm{N}\eta}\frac{\rho_{\eta\mathrm{N}}(s)}{\rho_{\eta\mathrm{N}}(M_{\mathrm{N}^*(1535)}^2)}, \tag{25}$$

where the two-body phase space factor $\rho_{\pi(\eta)\mathrm{N}}(s)$ is

$$\rho_{\pi(\eta)\mathrm{N}}(s) = \frac{\sqrt{[s-(m_{\mathrm{N}}+m_{\pi(\eta)})^2][s-(m_{\mathrm{N}}-m_{\pi(\eta)})^2]}}{s}$$

$$= \frac{2p_{\pi(\eta)\mathrm{N}}^{\mathrm{cm}}(s)}{\sqrt{s}}. \tag{26}$$

The invariant amplitude for the nucleon pole N or nucleon resonances N* can be expressed as

$$\mathcal{M}^{\mathrm{N/N}^*} = \sum_{i=\pi,\,\eta,\,\rho} \mathcal{M}_i^{\mathrm{N/N}^*}, \tag{27}$$

$$\mathcal{M}_i^{\mathrm{N/N}^*} = \sum_{j=a,\,b,\,c,\,d} \eta_j \mathcal{M}_{i,j}^{\mathrm{N/N}^*}, \tag{28}$$

where $\eta_a = \eta_d = 1$ and $\eta_b = \eta_c = -1$. The explicit expressions of $\mathcal{M}_{i,j}^{\mathrm{N/N}^*}$ can be derived straightforwardly according to the Feynman rules. For example, $\mathcal{M}_{\pi,a}^{\mathrm{N}^*(1535)}$ can be written as

$$\mathcal{M}_{\pi,a}^{\mathrm{N}^*(1535)} = g_{\pi\mathrm{NN}}g_{\pi\mathrm{NN}^*(1535)}g_{\eta\mathrm{NN}^*(1535)}F_\pi^{\mathrm{NN}}(k_\pi^2)$$

$$\times F_\pi^{\mathrm{N}^*(1535)\mathrm{N}}(k_\pi^2)F_{\mathrm{N}^*(1535)}(q^2)$$

$$\times G_\pi(k_\pi)\bar{u}(p_3,s_3)\gamma_5 u(p_2,s_2)\bar{u}(p_4,s_4)$$

$$\times G_{\mathrm{N}^*(1535)}(q)u(p_1,s_1), \tag{29}$$

where s_i ($i=1,2,3,4$) and p_i ($i=1,2,3,4$) represent the spin projection and 4-momentum of the two initial and two final protons, respectively.

The pp FSI and pη FSI are taken into account by introducing the following enhancement factors

$$F_{\mathrm{pp}}(k_{\mathrm{pp}}) = \frac{k_{\mathrm{pp}} + \mathrm{i}\beta}{k_{\mathrm{pp}} - \mathrm{i}\alpha}, \tag{30}$$

$$F_{\mathrm{p}\eta}(k_{\mathrm{p}\eta}) = \frac{1}{1 - \mathrm{i}k_{\mathrm{p}\eta}a}, \tag{31}$$

where k_{pp} and $k_{\mathrm{p}\eta}$ are the internal momenta of the pp and pη subsystems, respectively. The relevant parameters are: $\alpha = 0.1$ fm^{-1}, $\beta = 0.5$ fm^{-1} [55], and

$a = (0.487+\mathrm{i}0.171)$ fm [52, 53]. The overall final state interaction is the product of these enhancements [29, 55]:

$$F_{\mathrm{FSI}} = F_{\mathrm{pp}}(k_{\mathrm{pp}})F_{\eta\mathrm{p}}(k_{\eta\mathrm{p3}})F_{\eta\mathrm{p}}(k_{\eta\mathrm{p4}}), \qquad (32)$$

where p_3 and p_4 denote the two final protons.

With the modular square of the full invariant amplitude $|\mathcal{M}|^2 = \sum\limits_{\mathrm{N,N^*}} |\mathcal{M}^{\mathrm{N/N^*}} F_{\mathrm{FSI}}|^2$, the differential cross section for the pp→ppη reaction can be written as

$$\mathrm{d}\sigma(\mathrm{pp}{\to}\mathrm{pp}\eta) = \frac{1}{4}\frac{m_{\mathrm{p}}^2}{F}\sum_{s_i}\sum_{s_f}|\mathcal{M}|^2 \frac{m_{\mathrm{p}}\mathrm{d}^3 p_3}{E_3}\frac{m_{\mathrm{p}}\mathrm{d}^3 p_4}{E_4}$$

$$\times \frac{\mathrm{d}^3 p_5}{2E_5}\frac{1}{2}\delta^4(p_1+p_2-p_3-p_4-p_5), \quad (33)$$

where F is the flux factor

$$F = (2\pi)^5 \sqrt{(p_1 \cdot p_2)^2 - m_{\mathrm{p}}^4}. \qquad (34)$$

The factor $\dfrac{1}{2}$ before the δ function in Eq. (33) comes from the two identical protons in the final states. The interference terms between different resonances are ignored.

3   Numerical results and discussions

With a Monte Carlo multi-particle phase space integration program, the total cross section versus excess energy ε up to 80 MeV, the invariant mass spectra, angular distributions, and Dalitz plots at excess energies ε=15, 40, 57, and 72 MeV for the pp→ppη reaction are calculated.

The total cross section is shown in Fig. 2 together with the experimental data. Our results agree fairly well with the experimental data. From Fig. 2, one can see that the contributions from the t-channel ρ and π-meson exchanges are important and the ρ exchange plays the dominant role, but the contribution from the η-meson exchange is negligible. Figure 2 also shows that the contributions from the N*(1720) and N*(1535) are important and the N*(1720) plays the dominant role. The contribution of the N*(1535) is smaller than that of the N*(1720) due to the strong destructive interference among the exchange mesons, which is similar to the result of Ref. [33]. The contributions from the N*(1650) and N*(1710) are negligible.

The invariant mass spectra, angular distribution, and Dalitz plot at excess energy ε=15 MeV are shown in Fig. 3 together with experimental data. The measured pp and pη invariant mass spectra and the angular distribution of η are reproduced well. From Fig. 3 (a) and (d), one can see that the pp FSI plays an important role.

The invariant mass spectra, angular distribution, and Dalitz plot at excess energy ε=40 MeV as well as the experimental data are shown in Fig. 4. For the invariant mass spectra of proton–proton and proton–η, the theore-
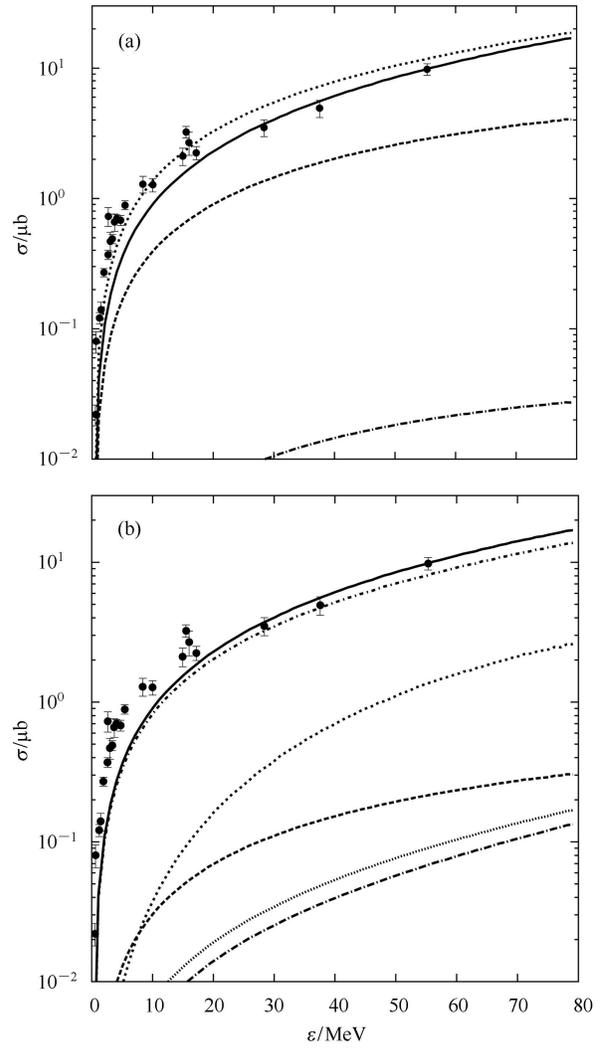
Fig. 2.   Total cross section vs excess energy ε for the pp → ppη reaction from the present calculation (solid curves) are compared with experimental data [2–7, 56–59]. (a) The dashed, dotted, and dashed-dotted lines stand for contributions from the π, ρ, and η-meson exchanges, respectively; (b) The dashed, dotted, short-dotted, dashed-dotted, and dot-short-dashed lines stand for contributions from the N, N*(1535), N*(1650), N*(1710), and N*(1720), respectively.

tical results are in agreement with the experimental data except for those near the proton–proton (proton–η) threshold. This small discrepancy indicates the pp FSI used in our calculation may be somewhat strong in this region.

For the angular distribution of the emitted η meson in the overall c.m. frame, there are two groups of data which do not agree with each other [8, 57]. One is isotropic [57], while the other is anisotropic [8], as shown in Fig. 4(c). Our result indicates that the angular distribution of the η meson is anisotropic, consistent with
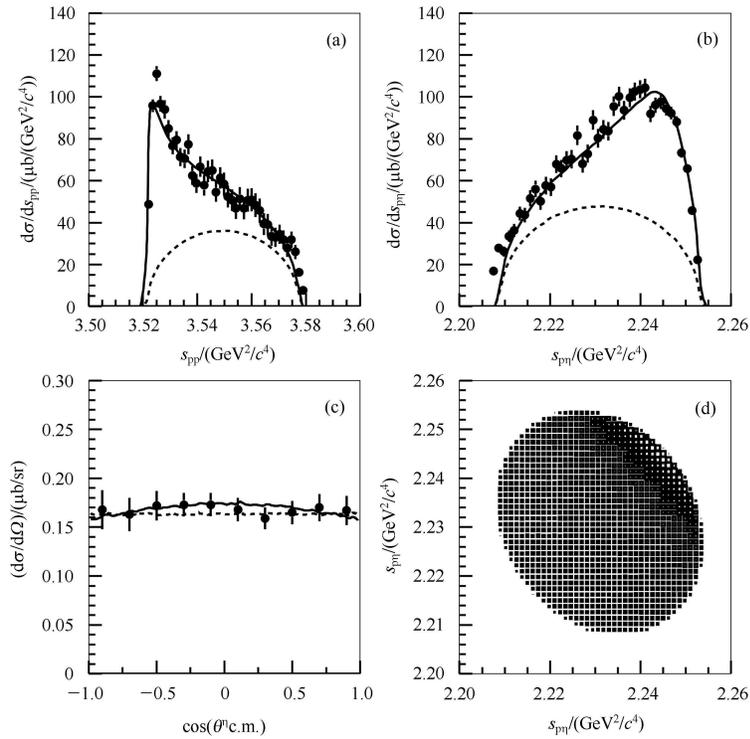
Fig. 3.   Differential cross sections (solid lines) and Dalitz plot for the pp→ppη reaction at the excess energy of ε=15 MeV compared with the experimental data [56, 57] and phase space distribution (dashed lines). (a) Distribution of the square of proton–proton invariant mass; (b) Distribution of the square of proton–η invariant mass; (c) Angular distribution of the emitted η meson in the c.m frame of the total system; (d) Dalitz plot.
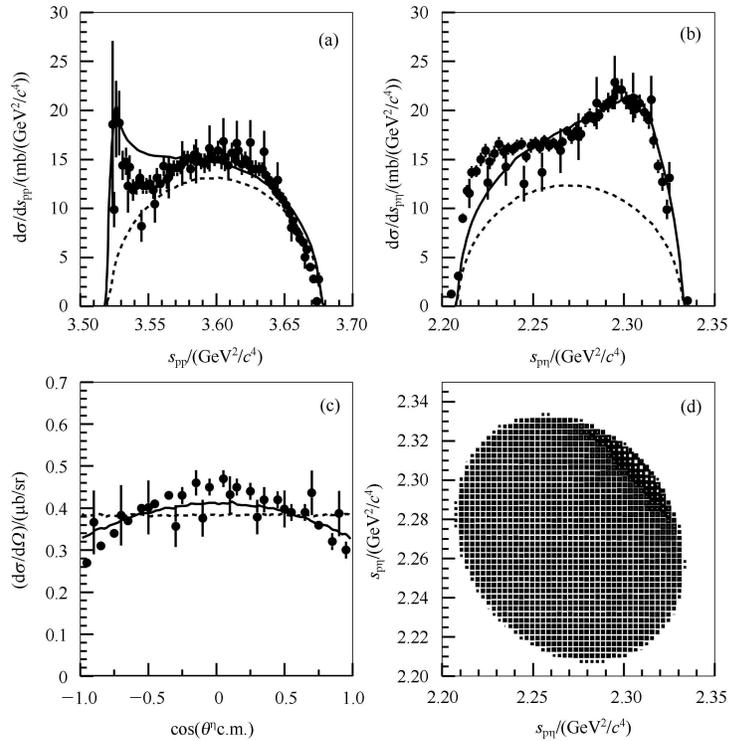
Fig. 4.   Same as Fig. 3 but at excess energy of ε=40 MeV. Experimental data are taken from Ref. [57] (squares) and Ref. [8] (dots).

the data from Ref. [8]. As pointed out by Refs. [8, 17, 58], the anisotropy is probably due to a mainly destructive interference between the dominant ρ exchange and π exchange. It is interesting to point out that the N*(1535) dominant interpretations [22, 28, 60] give almost isotropic angular distribution of the η at this region except that Ref. [27] gives the anisotropic angular distribution of the η by allowing for contributions from baryonic and mesonic currents.

The invariant mass spectra, angular distribution, and Dalitz plot at excess energy ε=72 MeV as well as the experimental data are shown in Fig. 5. The experimental data shown in Fig. 5 (a) indicate the pp FSI should be rather weak, so the pp FSI is ignored in this energy region. This rough procedure has been used in double-pion production in nucleon–nucleon collisions and the results turn out to be considerably improved [61]. Our pp invariant mass spectrum can reasonably account for the data.

The two-peak structure in the proton–η distribution cannot be reproduced in our calculation, which is similar to the result from Ref. [33]. This suggests that the structure in the pη distribution cannot be simply interpreted by the N*(1535), N*(1650), N*(1710), and N*(1720) resonances, and a more complicated mechanism is strongly called for.

Our angular distribution of the η at ε=72 MeV again indicates that the η distribution is anisotropic, consistent with the data from Ref. [8]. To our knowledge, there is as yet no theoretical paper for addressing the angular distribution of the η at this region.

The invariant mass spectra, angular distribution, and Dalitz plot at excess energy ε=57 MeV as well as preliminary experimental data are shown in Fig. 6. Similar to the case at excess energy ε=72 MeV, the preliminary data of Ref. [62] show that the two-peak structure appears in the proton-η distribution and the angular distribution of the η is anisotropic. Our predicted angular distribution for the η at ε=57 MeV is anisotropic, consistent with the data. However, the pη invariant mass distribution shows large differences between the present model and the experimental data.

It is noted that our present model does not include the higher partial waves for the pη FSI. As pointed out by Refs. [8, 63], the experimental data indicate the higher partial waves at higher reaction energies could be important. The contributions of the higher partial waves being ignored in the current model calculations may cause the discrepancy between the experimental data and our model of the proton–η distribution at excess energies ε=57 and 72 MeV.
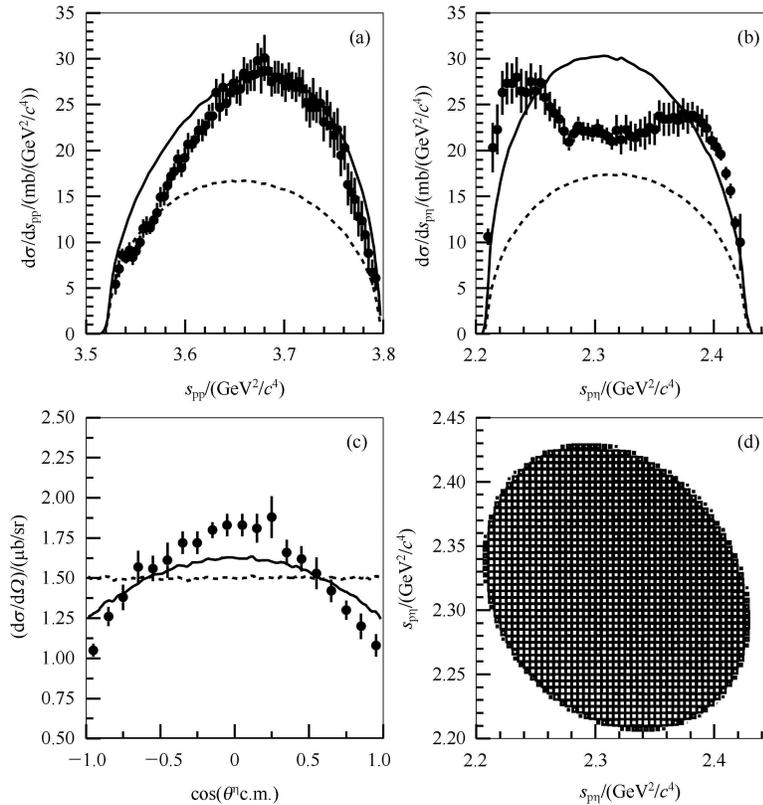
Fig. 5. Same as Fig. 3 but at excess energy of ε=72 MeV, and with pp FSI ignored. Experimental data are taken from Ref. [8].
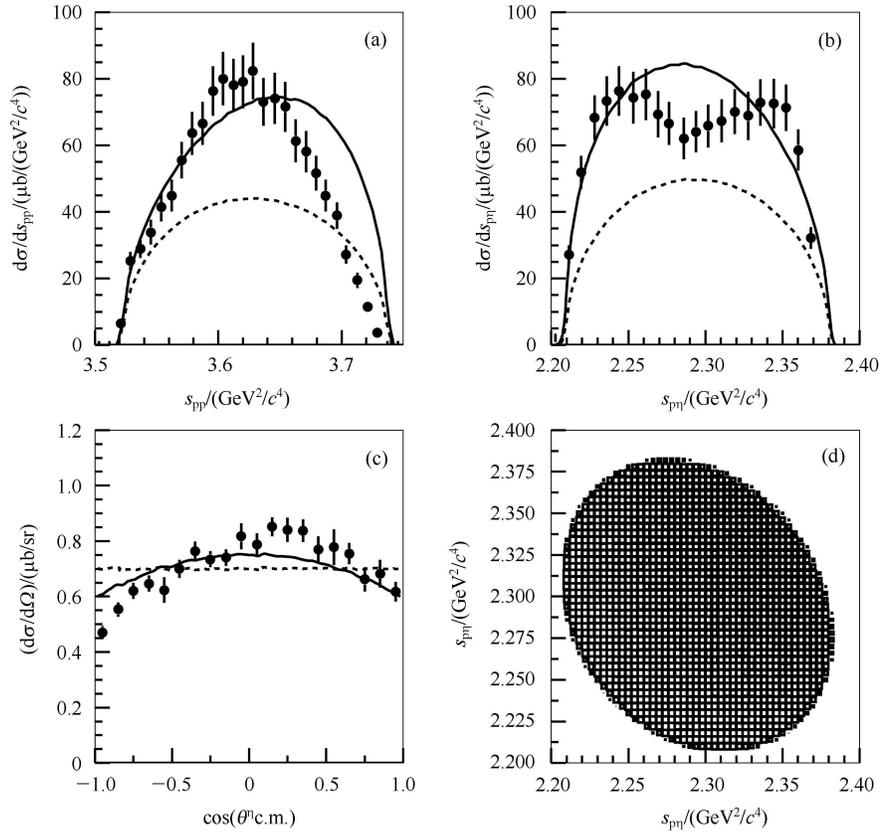
Fig. 6.   Same as Fig. 3 but at excess energy of ε=57 MeV, and with pp FSI ignored. Experimental data are taken from Ref. [62].

4   Summary and conclusions

In this paper we have calculated the pp$\rightarrow$ppη reaction within an effective Lagrangian approach combined with the isobar model. Our model calculations can reasonably reproduce the total cross sections up to excess energy of 80 MeV.

It is shown that for the pp$\rightarrow$ppη reaction, the contribution of the ρ-meson exchange is larger than that of the π-meson exchange, and the contribution of the N*(1720) is larger than that of the N*(1535).

Also, the same cut-off parameters for the N*(1650), N*(1710), and N*(1720) resonances are used, which makes it suitable to investigate the relative contributions of the N*(1650), N*(1710), and N*(1720) reso-

nances. Our results show that the contributions from the N*(1650) and N*(1710) are negligible.

Our calculations can reasonably explain the measured pp and pη invariant mass spectra at excess energies ε=15 and 40 MeV, but fail to explain the two-peak structure in the proton–η distribution at excess energies ε=57 and 72 MeV, which suggests that in the higher energy region, a more complicated mechanism is needed.

We give the anisotropic angular distribution of the η at ε=40, 57 and 72 MeV, consistent with the data from Refs. [8, 62]. This favors the interpretation that the interference between the ρ exchange and π exchange is mainly destructive.

References

1 Hanhart C. Phys. Rept., 2004, **397**: 155
2 Bergdolt A M, Bergdolt G, Bing O et al. Phys. Rev. D, 1993, **48**: 2969
3 Chiavassa E, Dellacasa, De Marco N et al. Phys. Lett. B, 1994, **322**: 270
4 Calén H, Carius S, Fransson K et al. Phys. Lett. B, 1996, **366**: 39
5 Hibou F, Bing O, Boivin M et al. Phys. Lett. B, 1998, **438**: 41
6 Smyrski J, Wuestner P, Budzanowski A et al. Phys. Lett. B, 2000, **474**: 182
7 Agakishiev G et al. (HADES collaboration). Eur. Phys. J. A, 2012, **48**: 74
8 Petrén H Bargholtz C, Bashkanov M et al. Phys. Rev. C, 2010, **82**: 055206
9 Czyżykiewicz R, Moskal P, Adam H et al. Phys. Rev. Lett., 2007, **98**: 122003
10 Pauly C. Light Meson Prodcution in pp Reactions at CELSIUS/WASA above the η Threshold (Ph. D. thesis). Hamburg: University of Hamburg, 2006
11 Calén H, Dyring J, Gustafsson K et al. Phys. Rev. Lett., 1997, **79**: 2642
12 Calén H, Dyring J, Gustafsson K et al. Phys. Rev. C, 1998, **58**: 2667
13 Calén H, Dyring J, Gustafsson K et al. Phys. Rev. Lett., 1998, **80**: 2069
14 Moskal P, Czyżykiewicz R, Adam H et al. Phys. Rev. C, 2009, **79**: 015208
15 Batinić M, Svarc A, Lee T S H. Phys. Scripta, 1997, **56**: 321
16 Moalem A, Gedalin E, Razdolskaya L et al. Nucl. Phys. A, 1996, **600**: 445
17 Germond J F, Wilkin C. Nucl. Phys. A, 1990, **518**: 308
18 Laget J M, Wellers F, Lecolley J F. Phys. Lett. B, 1991, **257**: 254
19 Vetter T, Engel A, Biró T et al. Phys. Lett. B, 1991, **263**: 153
20 Alvaredo B L, Oset E. Phys. Lett. B, 1994, **324**: 125
21 Pena M T, Garcilazo H, Riska D O. Nucl. Phys. A, 2001, **683**: 322
22 Shyam R. Phys. Rev. C, 2007, **75**: 055201
23 Gedalin E, Moalem A, Razdolskaya L. Nucl. Phys. A, 1998, **634**: 368
24 Santra A B, Jain B K. Nucl. Phys. A, 1998, **634**: 309
25 Fäldt G, Wilkin C. Phys. Scripta, 2001, **64**: 427
26 Baru V, Gasparyan, Haidenbauer et al. Phys. Rev. C, 2003, **67**: 024002
27 Nakayama K, Speth J, Lee T S H. Phys. Rev. C, 2002, **65**: 045210
28 Nakayama K, Haidenbauer J, Hanhart C et al. Phys. Rev. C, 2003, **68**: 045201
29 Bernard V, Kaiser N, Meissner Ulf-G. Eur. Phys. J. A, 1999, **4**: 259
30 Moskal P, Wolke M, Khoukaz A et al. Prog. Part. Nucl. Phys., 2002, **49**: 1
31 Riska D O, Brown G. Nucl. Phys. A, 2001, **679**: 577
32 CAO X, Lee X G. Phys. Rev. C, 2008, **78**: 035207
33 Nakayama K, Oh Y, Haberzettl H. J. Korean Phys. Soc, 2011, **59**: 224
34 Deloff A. Phys. Rev. C, 2004, **69**: 035206
35 XIE J J, Wilkin C, ZOU B S. Phys. Rev. C, 2008, **77**: 058202
36 XIE J J, ZOU B S. Phys. Lett. B, 2007, **649**: 405
37 XIE J J, ZOU B S, Chaing H Q. Phys. Rev. C, 2008, **77**: 015206
38 LÜ Q F, LIU X H, XIE J J et al. Mod. Phys. Lett. A, 2014, **29**: 1450012
39 LÜ Q F, XIE J J, LI D M. Phys. Rev. C, 2014, **90**: 034002
40 LÜ Q F, WANG R, XIE J J et al. Phys. Rev. C, 2015, **91**: 035204
41 Machleidt R, Holinde K, Elster C. Phys. Rep., 1987, **149**: 1
42 Machleidt R. Adv. Nucl. Phys., 1989, **19**: 189
43 Brockmann R, Machleidt R, Phys. Rev. C, 1990, **42**: 1965
44 Tsushima K, HUANG S W, Faessler A. Phys. Lett. B, 1994, **337**: 245
45 Tsushima K, Sibirtsev A, Thomas A W. Phys. Lett. B, 1997, **390**: 29
46 Tsushima K, Sibirtsev A, Thomas A W et al. Phys. Rev. C, 1999, **59**: 369; Erratum-ibid. C, 2000, **61**: 029903
47 Sibirtsev A, Cassing W. arXiv:nucl-th/9802019
48 Sibirtsev A, Tsushima K, Cassing W et al. Nucl. Phys. A, 1999, **646**: 427
49 ZOU B S, Hussain F. Phys. Rev. C, 2003, **67**: 015204
50 Olive K A et al. (Particale Data Group). Chin. Phys. C, 2014, **38**: 090001
51 Penner G, Mosel U. Phys. Rev. C, 2002 **66**: 055211; 055212; Shklyar V, Lenske H, Mosel U. Phys. Rev. C, 2005, **72**: 015210
52 Feuster T, Mosel U, Phys. Rev. C, 1998, **58**: 457
53 Feuster T, Mosel U. Phys. Rev. C, 1999, **59**: 460
54 LIANG W H, SHEN P N, WANG J X et al. J. Phys. G, 2002, **28**: 333
55 Maeda Y et al. (ANKE collaboration). Phys. Rev. C, 2008, **77**: 015204
56 Moskal P, Adm H H, Budzanowski A et al. Phys. Rev. C, 2004, **69**: 025203
57 Abdel-Bary M et al. (COSY-TOF collaboration). Eur. Phys. J. A, 2003, **16**: 127
58 Calen H, Dyring J, Fransson K et al. Phys. Lett. B, 1999, **458**: 190
59 Balestra F, Bedfer Y, Bertini R et al. Phys. Rev. C, 2004, **69**: 064003
60 Fix A, Arenhoevel H. Phys. Rev. C, 2004, **69**: 014001
61 CAO X, ZOU B S, XU H S. Phys. Rev. C, 2010, **81**: 065201
62 Shah N. AIP Conf. Proc, 2011, **1374**: 402
63 Krusche B, Wilkin C. Prog. Part. Nucl. Phys, 2014, **80**: 43